

1 **Article Title: Metabolic modelling of the C₃-CAM continuum revealed the**
2 **establishment of a starch/sugar-malate cycle in CAM evolution**

3

4 Ignacius Tay Y. Y.¹, Kristoforus Bryant Odang¹ and C. Y. Maurice Cheung*¹

5

6 ¹Yale-NUS College, 16 College Avenue West, Singapore 138527

7

8 *Corresponding author: C. Y. Maurice Cheung

9 Telephone: +65 66015276

10 Email: maurice.cheung@yale-nus.edu.sg

11

12 Running Title: Metabolic modelling of the C₃-CAM continuum

13 **Abstract**

14 The evolution of Crassulacean acid metabolism (CAM) is thought to be along a C₃-CAM
15 continuum including multiple variations of CAM such as CAM cycling and CAM idling. Here,
16 we applied large-scale constraint-based modelling to investigate the metabolism and energetics
17 of plants operating in C₃, CAM, CAM cycling and CAM idling. Our modelling results suggested
18 that CAM cycling and CAM idling could be potential evolutionary intermediates in CAM
19 evolution by establishing a starch/sugar-malate cycle. Our model analysis showed that by
20 varying CO₂ exchange during the light period, as a proxy of stomatal conductance, there exists a
21 C₃-CAM continuum with gradual metabolic changes, supporting the notion that evolution of
22 CAM from C₃ could occur solely through incremental changes in metabolic fluxes. Along the
23 C₃-CAM continuum, our model predicted changes in metabolic fluxes not only through the
24 starch/sugar-malate cycle that is involved in CAM photosynthetic CO₂ fixation but also other
25 metabolic processes including the mitochondrial electron transport chain and the tricarboxylate
26 acid cycle at night. These predictions could guide engineering efforts in introducing CAM into
27 C₃ crops for improved water use efficiency.

28

29 Key words

30 CAM cycling, CAM evolution, CAM idling, Crassulacean acid metabolism, metabolic
31 modelling, flux balance analysis

32 **Introduction**

33 Crassulacean acid metabolism (CAM) photosynthetic CO₂ fixation is an evolutionary
34 descendant of C₃ photosynthesis, which is known to have evolved independently multiple times
35 in at least 35 plant families comprising about 6% of flowering plant species (Winter and Smith,
36 1996a; Silvera et al., 2010). CAM is an adaptation of photosynthetic CO₂ fixation typically
37 associated to limited water availability (Cushman and Borland, 2002). By closing their stomata
38 during the light period and fixing atmospheric and/or respiratory carbon dioxide (CO₂)
39 exclusively in the dark period, CAM allows plants to use water more efficiently while fixing
40 carbon for growth. The engineering of CAM into C₃ crops has been suggested as a possible
41 strategy to meet the demands on agriculture for food, feed, fibre, and fuels, without exacerbating
42 the pressures on arable land area due to climate change (Borland et al., 2014). However, as a
43 carbon-concentrating mechanism, CAM is thought to be more metabolically expensive than C₃
44 (Winter and Smith, 1996b), which suggests that transferring a CAM pathway into C₃ crops
45 would incur a crop yield penalty. To investigate the energetics of C₃ and CAM, large-scale
46 metabolic models were applied which showed that engineering CAM into C₃ plants does not
47 impose a significant energetic penalty given the reduction in photorespiration from the carbon-
48 concentrating mechanism (Cheung et al., 2014; Shameer et al., 2018).

49 Besides the phylogenetic and ecological diversity of CAM plants, there is remarkable
50 plasticity in its metabolism with multiple defined variations of CAM including CAM cycling and
51 CAM idling (Ting, 1985; Cushman, 2001, Winter, 2019). Briefly, CAM cycling primarily fixes
52 CO₂ in the light period with refixing respiratory CO₂ behind closed stomata at night, leading to a
53 small diel organic acid flux; CAM idling lacks diel gaseous exchange with closed stomata across
54 the 24 hour light/dark cycle and has a small continued diel fluctuation in organic acids level
55 (Sipes and Ting, 1985; Cushman, 2001, Winter, 2019). Silvera et al. (2010) generalised the idea
56 of plasticity of CAM into a continuum of CAM levels, due to the differences in the degree of
57 nocturnal and daytime net CO₂ uptake. Bräutigam et al. (2017) took the idea further to include C₃
58 as part of the C₃-CAM continuum and suggested that the evolution of C₃ to CAM only required
59 incremental increases in metabolic fluxes. In this study, large-scale metabolic modelling was
60 applied to investigate how CAM cycling and CAM idling fit into the continuum of CAM
61 evolution and to identify the changes in metabolic fluxes along the C₃-CAM continuum. The

62 results from our modelling study provide novel insights into the energetics and metabolic
63 alterations from C₃ to CAM, which could guide engineering efforts aimed at introducing CAM
64 into C₃ plants.

65

66 **Materials and Methods**

67 **Core metabolic model for modelling C₃, CAM, CAM cycling and CAM idling**

68 The mass- and charge-balance core metabolic model of Arabidopsis in Shameer et al.
69 (2018) was used for modelling the metabolism of leaves operating in C₃, CAM, CAM cycling
70 and CAM idling. A number of minor modifications were made to the Shameer et al. (2018)
71 model to more accurately model metabolism of C₃, CAM, CAM cycling, CAM idling and the
72 C₃-CAM continuum. Firstly, a reaction for the accumulation of oxygen, which is produced from
73 water splitting in the photosynthetic light reactions, was added to the model such that we could
74 run the simulations for CAM and CAM idling as oxygen exchange was constrained to zero
75 during the day in these two scenarios. Another modification from Shameer et al. (2018) was how
76 the acidification of the vacuole was modelled. Instead of directly setting different fixed pH for
77 the vacuole in C₃ and CAM, protons were allowed to accumulate in the vacuole in our model. A
78 reaction allowing protons to freely flow in and out of the cytosol was blocked such that pH
79 homeostasis can be modelled through the accumulation of protons in the vacuole. For linking the
80 cytosolic and mitochondrial proton pools, proton transport between the cytosol and the
81 mitochondrial intermembrane space was set to be reversible. The modification of this constraint
82 only led to a very minor change in the flux predictions (data not shown). Irreversible proton
83 transporters were added from the vacuole to the cytosol and from extracellular to the cytosol to
84 allow leakage of protons down the electrochemical gradients. Lastly, the compartmentation of
85 metabolites in the reaction “HEXOKINASE_RXN_MANNOSE_c” was corrected to be in the
86 cytosol. The modified core model can be found in SBML and Excel formats (Supplementary File
87 S1).

88

89 **Model simulations with flux balance analysis**

90 Based on the constraints and objective function stated in the Results section, parsimonious flux
91 balance analysis (pFBA) was performed using scobra (<https://github.com/mauriceccy/scobra>), an
92 extension of cobrapy (Ebrahim et al., 2013). The scripts for running the simulations in this study
93 can be found in Supplementary File S2. In this study, we primarily reported the results from the
94 pFBA simulations (Supplementary Tables S1, S2, S3). The conclusions made based on the pFBA
95 results for C₃, CAM, CAM cycling and CAM idling were confirmed using flux variability
96 analysis (Mahadevan and Schilling, 2003) applied on the primary objective (Supplementary
97 Table S4).

98

99 **Results**

100 **Predicted metabolic fluxes of C₃, CAM, CAM cycling and CAM idling**

101 In this study, we simulated the metabolism of leaves undergoing C₃, CAM, CAM cycling
102 and CAM idling using a recently published core metabolic model of Arabidopsis which was used
103 to model C₃ and CAM plants (Shameer et al., 2018). Minor modifications of the model were
104 outlined in the Materials and Methods section. The constraints for simulating the core metabolic
105 functions of mature leaves, namely export of sucrose and amino acids into the phloem and
106 cellular maintenance, were set based on the values in Shameer et al. (2018). All simulations,
107 except CAM idling, were constrained to have a phloem export rate of 0.259 $\mu\text{mol m}^{-2} \text{s}^{-1}$ based
108 on the value of C₃ plants in Shameer et al. (2018). The set of constraints for modelling the four
109 different modes of photosynthesis are summarised in Table 1. The primary objective function of
110 minimising photon demand was used throughout this study, which allows us to study the
111 metabolic efficiencies of the different modes of photosynthesis. Parsimonious flux balance
112 analysis (pFBA), i.e. minimisation of absolute sum of fluxes, was applied as a secondary
113 objective to eliminate substrate cycles. Results from pFBA were confirmed using flux variability
114 analysis (Mahadevan and Schilling, 2003) performed on the primary objective.

115 The model predictions of C₃ and CAM were very similar to that in Shameer et al. (2018)
116 given the similarities in the constraints used. Without any constraints on malate decarboxylation
117 enzyme and carbohydrate storage, the model predicted net carbon fixation during the light period

118 in the C₃ flux prediction, whereas in CAM carbon was fixed in the dark period with
119 phosphoenolpyruvate carboxykinase (PEPCK) being the main predicted route for malate
120 decarboxylation. Starch was predicted to be the main carbohydrate storage in both C₃ and CAM.
121 These results are consistent with the findings in Shameer et al. (2018) where starch-storing
122 PEPCK subtype were predicted to be the most energy efficient. The effect of the choice of
123 decarboxylation enzymes (PEPCK vs malic enzyme) on the model predictions was explored by
124 constraining other decarboxylating enzymes to carry zero flux. It was found that the choice of
125 decarboxylation enzymes makes little qualitative difference with respect to the results presented
126 (Supplementary Table S5). From here on, the results presented were model predictions with no
127 constraints on the decarboxylation enzymes. As for carbohydrate storage, simulations were
128 performed with starch, sucrose or fructan as the sole carbohydrate storage. Except for reactions
129 involved in the synthesis, accumulation and degradation of carbohydrate storage, the predicted
130 fluxes in central carbon metabolism were largely similar between the three carbohydrate storages
131 tested (Supplementary Table S6). In this study, we mostly presented the results from simulations
132 with starch as the carbohydrate storage. Similar conclusions can be made for using sugar as the
133 carbohydrate storage. The core set of metabolic fluxes for C₃, CAM, CAM cycling and CAM
134 idling with starch as the carbohydrate storage is depicted in Figure 1.

135 ***CAM cycling***

136 Similar to C₃ plants, CAM cycling fixes carbon in the light period. CAM cycling is
137 characterised by its closed stomata in the dark period with re-fixation of respiratory CO₂ and a
138 small diel organic acid flux (Sipes and Ting, 1985; Cushman, 2001, Winter, 2019). To model
139 CAM cycling, we applied the C₃ constraints with an additional constraint of setting CO₂ and O₂
140 exchange at night to zero to simulate the closure of the stomata (Table 1). This resulted in a flux
141 distribution that resembled a weak version of CAM, with nocturnal malate accumulation and
142 increased light period starch accumulation (Figure 1C). Phosphoenolpyruvate carboxylase
143 (PEPC) was predicted to be active only at night in CAM cycling for CO₂ re-fixation, in contrast to
144 C₃ where PEPC was only active during the light period (Supplementary Table S2). Another
145 major difference between CAM cycling and C₃ is malate accumulation. While C₃ was predicted
146 to have a very small amount of malate accumulation during the light period, CAM cycling was
147 predicted to have substantial amount of nocturnal malate accumulation (~20% of the amount of
148 malate accumulation in CAM) (Figure 1; Supplementary Table S2), which is consistent with

149 known behaviour of CAM cycling (Ting, 1985; Cushman, 2001). The nocturnal malate
150 accumulation and respiratory CO₂ refixation via PEPC under the CAM cycling scenario were
151 accompanied by changes in fluxes in other parts of metabolism. Malate decarboxylation during
152 the light period was predicted to be active in CAM cycling but not in C₃ (Figure 1). There was a
153 larger flux through gluconeogenesis to convert malate into starch in the light period, which led to
154 more starch accumulation during the light period in CAM cycling compared to C₃ (Figure 1;
155 Supplementary Table S2). Given that CAM cycling has a higher starch accumulation in the light
156 period, it was predicted to have a larger glycolytic flux in the dark to convert starch into
157 phosphoenolpyruvate (PEP) for CO₂ refixation, compared to C₃ (Figure 1; Supplementary Table
158 S2). The activities of most of the other reactions at night were similar in CAM cycling and in C₃,
159 with CAM cycling having a slightly higher flux through the tricarboxylic acid (TCA) cycle and
160 the mitochondrial electron transport chain (ETC), presumably to produce extra ATP for
161 transporting malate into the vacuole for storage at night.

162 ***CAM idling***

163 CAM idling is characterised by the lack of diel gaseous exchange and a small continued
164 diel fluctuation in the organic acids level because of internally recycled CO₂ (Sipes and Ting,
165 1985, Winter, 2019). It is usually an adaptation in water-stressed plants, which results in the
166 closure of stomata for the whole 24-hour cycle. To model this, the CO₂ and O₂ exchange during
167 the light and the dark periods were constrained to carry zero flux (Table 1). Given that there is no
168 CO₂ exchange, we assumed that there is no net carbon fixation, hence phloem export was
169 constrained to zero for CAM idling.

170 The primary metabolic demand for plants in CAM idling is cellular maintenance. The
171 model predicted a starch-malate cycle where starch accumulated in the light period is
172 metabolised in the dark period mainly through glycolysis and the oxidative pentose phosphate
173 pathway (OPPP) to produce ATP and NADPH for maintenance processes (Figure 1D). While the
174 majority of PEP was used as precursor for carbon refixation by PEPC, a significant proportion of
175 PEP was predicted to be metabolised further through the TCA cycle to feed the mitochondrial
176 ETC for ATP synthesis (Figure 1D). Given that it is a closed system with respect to carbon, CO₂
177 produced in the OPPP and the TCA cycle is refixed by PEPC, which ultimately leads to the
178 accumulation of malate in the dark. In the light period, PEP from malate decarboxylation was

179 recycled to produce starch via gluconeogenesis, while the CO₂ produced from malate
180 decarboxylation was refixed via the Calvin-Benson cycle similar to the scenario for CAM
181 (Figure 1). With no net carbon import or export, the amount of carbon stored in starch in the light
182 period was predicted to be equalled to the amount of carbon storage in malate at night. The
183 starch-malate cycle was primarily driven by the energy from the light reactions of
184 photosynthesis, and it acted as a carbon neutral way of storing and transferring energy from the
185 light period to the dark period. Similar results were obtained when sucrose or fructan was used as
186 the sole carbohydrate storage instead of starch (Supplementary Table S6), meaning that a sugar-
187 malate cycle can serve the same function as the starch-malate cycle in sugar-storing plants.

188

189 **Energetics and metabolite accumulation in C₃, CAM, CAM cycling and CAM** 190 **idling**

191 The metabolic flux predictions of C₃, CAM, CAM cycling and CAM idling were
192 compared to see how CAM cycling and CAM idling fit into the evolution of CAM from C₃.
193 Table 2 summarises the predicted fluxes related to energetics and metabolite accumulation in the
194 four simulations. CAM idling was predicted to use the fewest photons, which was expected
195 given that it does not have the metabolic demand for exporting sucrose and amino acids into the
196 phloem. For the same metabolic demand, CAM requires more photons than C₃, as expected. It is
197 interesting to see that the photon demand for CAM cycling falls between C₃ and CAM. A similar
198 trend was observed for other fluxes related to energy metabolism including the ATP and
199 NADPH production by the photosynthetic light reactions and the ATP production by the
200 mitochondrial ATP synthase (Table 2). The same trend was also reflected in the energetic
201 demands of the Calvin-Benson cycle in terms of ATP and NADPH consumption (Supplementary
202 Table S2).

203 Metabolite accumulation showed a different pattern compared to the energetics (Table 2).
204 C₃ had the lowest daytime starch accumulation, followed by CAM cycling and CAM idling
205 which had about 2-3 times more starch accumulation than C₃. CAM had the highest light period
206 starch accumulation with more than nine times the amount associated with C₃. This suggested
207 that CAM cycling and CAM idling could potentially be intermediate steps in CAM evolution

208 with respect to the regulation of starch accumulation. A similar pattern can be observed for
209 malate accumulation. A very small amount of malate was predicted to accumulate during the day
210 for C₃ plants, whereas a large nocturnal malate accumulation was predicted for CAM as part of
211 CAM photosynthesis. CAM cycling and CAM idling had intermediate level of nocturnal malate
212 accumulation (~20% of that in CAM), which was related to the refixation of nocturnal CO₂ by
213 PEPC. Reactions related to the starch/sugar-malate cycle, including glycolysis and PEPC flux in
214 the dark period, and gluconeogenesis and malate decarboxylation during the light period, showed
215 a similar trend (Supplementary Table S2) suggesting that CAM cycling and/or CAM idling could
216 be an evolutionary intermediate for the evolution of the extensive starch/sugar-malate cycle in
217 CAM plants.

218

219 **Predicting the metabolic transitions during C₃-CAM evolution**

220 The behaviour of diel CO₂ exchange is the main diagnostic indicator between C₃ and
221 CAM (Silvera et al., 2010). To model the potential metabolic transitions that could happen
222 during the evolution of CAM from C₃, we varied the CO₂ uptake rate during the light period
223 from 13.12 μmol m⁻² s⁻¹ (the predicted value for C₃) to 0 μmol m⁻² s⁻¹ (which had the same
224 effect as gradually increasing nocturnal CO₂ uptake given the overall carbon balance). This
225 simulates the decrease in gaseous exchange during the light period by stomatal closure, hence a
226 similar constraint was set for light period oxygen exchange. As the stomata closes in the light
227 period, i.e. light period CO₂ uptake decreases, it was assumed that the proportion of ribulose-1,5-
228 biphosphate carboxylase/oxygenase (RuBisCO) flux going through the carboxylase reaction
229 increases linearly from 75% (carboxylase to oxygenase ratio of 3:1) to 83.74% (carboxylase to
230 oxygenase ratio of 5.15:1) to account for the reduction of photorespiration. All other constraints
231 remained the same as the C₃ and CAM simulations. This analysis simulates the closing of
232 stomata which decreases atmospheric CO₂ intake during the light period. The full results from
233 this simulation can be found in Supplementary Table S3.

234 Given that the metabolic demands remained constant throughout the analysis, a decrease
235 in CO₂ uptake in the light period led to a shift from C₃ to CAM photosynthesis with an increase
236 in flux through the starch-malate cycle including starch degradation, glycolysis, PEPC, and
237 malate accumulation at night, and malate decarboxylation and starch accumulation during the

238 light period (Figure 2A,B; Supplementary Table S3). Note that dark period CO₂ uptake increased
239 as light period CO₂ uptake decreased due to the carbon balance of the model in exporting a fixed
240 amount of sucrose and amino acids into the phloem. CAM cycling occurs at the point when dark
241 period CO₂ uptake is zero.

242 Despite the constrained decrease in RuBisCO oxygenase contribution as light period
243 CO₂ uptake decreased, the amount of energy (in terms of photons) required to sustain the same
244 metabolic demand increased by about 7% from C₃ to CAM (Figure 2C) as extra energy is needed
245 to run the starch-malate cycle. This is correlated with the increase in flux through the
246 photosynthetic light reactions. Besides plastidial ATP synthesis, there was also an increase in
247 ATP synthesis by the mitochondrial ETC in the light period as the simulation shifted from C₃ to
248 CAM (Figure 2D). The contribution of mitochondrial ATP synthesis increased from 18.2% in C₃
249 to 35.6% in CAM (Figure 2E), which is likely to be related to the increase in NADH produced
250 during malate decarboxylation. In our simulations, the RuBisCO carboxylase flux was predicted
251 to remain relatively constant while the total RuBisCO flux (carboxylase + oxygenase)
252 decreased from C₃ to CAM due to the decrease in RuBisCO oxygenase activity (Figure 2F).
253 There were two major factors affecting RuBisCO carboxylase flux, i) refixation of
254 photorespiratory CO₂, and ii) starch accumulation to support energy demand in the dark period.
255 In this case, the two factors counteract each other throughout the simulation where
256 photorespiration decreases and the energy demand for running the starch-malate cycle (mostly
257 for pumping malate into the vacuole) increases from C₃ to CAM. For the simulations with
258 sucrose or fructan as the sole carbohydrate storage, the model predicted an increase in RuBisCO
259 carboxylase flux from C₃ to CAM as the energy required for running the sugar-malate cycle is
260 higher than the starch-malate cycle (due to the cost of pumping sugars into the vacuole for
261 storage).

262 During the night, other than the increase in glycolytic flux as part of the starch-malate
263 cycle from C₃ to CAM, the model predicted an 87% increase in flux through the TCA cycle and
264 an 83% increase in flux through the mitochondrial ETC (Figure 2G). This increase in
265 mitochondrial ATP synthesis was mostly used to support the ATP-dependent tonoplast proton
266 pump for the increasing nocturnal vacuolar malate accumulation. The cytosolic OPPP flux was
267 predicted to decrease by 30% in the night from C₃ to CAM (Figure 2h). This could be explained

268 by the increase in the TCA cycle flux which contributed to the production of NADPH in the
269 mitochondrion by the NADP-isocitrate dehydrogenase. This lessened the demand for the
270 production of cytosolic NADPH required to be shuttled into the mitochondrion for maintenance
271 processes.

272

273 **Discussion**

274 **CAM cycling and CAM idling as viable evolutionary steps for establishing the** 275 **starch-malate cycle**

276 CAM cycling is considered as a weak form of CAM with stomata are open during the day
277 and are closed at night (Lüttge, 2004; Silvera et al., 2010, Winter, 2019). With these constraints,
278 our model predicted the known features of CAM cycling including the refixation of respiratory
279 CO₂ in the dark period, and a small amount of nocturnal malate accumulation (Cushman, 2001,
280 Winter, 2019). To support these metabolic behaviours, our model predicted the establishment of
281 a starch-malate cycle in CAM cycling, which included increased flux through malate
282 decarboxylation, gluconeogenesis and starch synthesis and accumulation during the light period,
283 and starch degradation and glycolysis during the dark period, when compared to C₃ plants. The
284 main metabolic advantage of CAM cycling over C₃ is its higher carbon conversion efficiency
285 when photosynthesis is limited by stomatal conductance in the light period, i.e. carbon limited.
286 Given the same metabolic outputs, CAM cycling was predicted to require 20% less external CO₂
287 compared to C₃ due to the refixation of nocturnal respiratory CO₂. This comes with a minor cost
288 of 4.8% more photons and 1.6% more RuBisCO activity required, assuming that there is no
289 reduction in photorespiration, which could be affected by limiting stomatal conductance and
290 internal CO₂ generation from malate decarboxylation. Given an environment that limits stomatal
291 conductance in the light period, e.g. high temperature and drought, the evolution of CAM
292 cycling, together with the establishment of the starch/sugar-malate cycle, was predicted to be
293 advantageous in maximising carbon conversion efficiency. The metabolic activities of all
294 reactions in the starch-malate cycle in CAM cycling were predicted to be at an intermediate level
295 between C₃ and CAM. The same applies to other supporting reactions such as the TCA cycle in
296 the dark and the mitochondrial ETC during the light and dark periods. These findings suggest

297 that CAM cycling is likely to be a possible evolutionary step along the path to the evolution of
298 CAM.

299 As opposed to CAM cycling, CAM idling is thought of as a form of very strong CAM
300 (Lüttge, 2004, Winter, 2019). In CAM idling, stomata remain closed throughout the day and
301 night with small, sustained diel fluctuations in organic acids (Cushman, 2001; Silvera et al.,
302 2010, Winter, 2019). By constraining our model with closed stomata in both the light and dark
303 periods, the model predicted the operation of the starch/sugar-malate cycle as the most energy
304 efficient way to sustain cellular activities. From an evolutionary perspective, if a plant often
305 experiences conditions that require the closure of stomata throughout day and night, such as long
306 periods of severe drought, the evolution of CAM idling would be advantageous for the plant to
307 stay alive. While the evolution of CAM through CAM cycling seems more likely given its
308 similarities to C_3 , it is not impossible that some lineages could establish the starch/sugar-malate
309 cycle through CAM idling.

310

311 **Stomatal conductance as a determinant along the C_3 -CAM continuum**

312 It has been proposed that CAM evolution occurs along a continuum from C_3 to CAM
313 (Silvera et al., 2010; Bräutigam et al., 2017). Our model analysis showed that by varying the CO_2
314 exchange in the light period, as a proxy for stomatal conductance, there existed a C_3 -CAM
315 continuum with gradual metabolic changes along the continuum (Figure 2). The key metabolic
316 changes included the processes in the starch/sugar-malate cycle, the TCA cycle at night, and the
317 chloroplastic and mitochondrial ETCs. The fact that a gradual continuum was predicted to be the
318 most energetically favourable way to adapt to a change in stomatal conductance suggests that the
319 fitness landscape between C_3 and CAM is a smooth one. Given our results, it is not surprising to
320 see many facultative CAM plants which can easily switch between C_3 and CAM. Based on our
321 model predictions, it is hypothesised that we could find plants anywhere on the C_3 -CAM
322 continuum. A prime example is CAM cycling which falls within the C_3 -CAM continuum at the
323 point when nocturnal CO_2 exchange is zero. Given the flexibility shown in facultative CAM
324 plants and our results on the C_3 -CAM continuum, it could be possible to find existing plants or
325 engineer new plants that can switch not only between C_3 and CAM but also at different points on
326 the continuum depending on the environmental conditions.

327

328 **Conclusion**

329 Using a core metabolic model of Arabidopsis, we were able to model the metabolic
330 behaviours of CAM, CAM cycling and CAM idling by changing a few simple constraints on
331 gaseous exchange and phloem export. Our results showed that CAM cycling and CAM idling
332 could potentially be evolutionary intermediates on the path to CAM evolution by establishing an
333 intermediate flux through the starch/sugar-malate cycle. By varying the light period CO₂
334 exchange as a proxy for stomatal conductance, the model predicted a continuum from C₃ to
335 CAM with gradual metabolic changes. Besides the insights gained in CAM evolution, the results
336 from this study are informative to guide engineering efforts aiming to introduce CAM into C₃
337 crops by identifying the metabolic changes required to convert C₃ to CAM. In addition to the
338 starch/sugar-malate cycle involved in CAM photosynthesis, our model showed that the fluxes of
339 other metabolic processes, including the TCA cycle and the mitochondrial ETC, need to be
340 altered from C₃ to optimise CAM.

341

342 **List of Supplementary Data**

343 **Supplementary File S1:** Core metabolic model for simulating C₃, CAM, CAM cycling and
344 CAM idling in SBML and Excel formats

345 **Supplementary File S2:** Python scripts for running model simulations

346 **Supplementary Table S1:** Flux solutions from parsimonious flux balance analysis for C₃, CAM,
347 CAM cycling and CAM idling

348 **Supplementary Table S2:** A summary of predicted fluxes of key reactions in central
349 metabolism from parsimonious flux balance analysis for C₃, CAM, CAM cycling and CAM
350 idling

351 **Supplementary Table S3:** Flux solutions from parsimonious flux balance analysis for the C₃-
352 CAM continuum

353 **Supplementary Table S4:** Flux ranges from flux variability analysis for C₃, CAM, CAM
354 cycling and CAM idling

355 **Supplementary Table S5:** Model flux predictions with different malate decarboxylating
356 enzymes

357 **Supplementary Table S6:** Model flux predictions with different carbohydrate storage

358

359 **Acknowledgements**

360 We thank Yale-NUS College (WBS R-607-265-233-121) for the financial support.

361

References

Borland AM, Hartwell J, Weston DJ, Schlauch KA, Tschaplinski TJ, Tuskan GA, Yang X, Cushman JC. 2014. Engineering crassulacean acid metabolism to improve water-use efficiency. *Trends in Plant Science* 19, 327–338.

Bräutigam A, Schlüter U, Eisenhut M, and Gowik U. 2017. On the Evolutionary Origin of CAM Photosynthesis. *Plant Physiology* 174, 473–477.

- Cheung CYM, Poolman MG, Fell DA, Ratcliffe RG, Sweetlove LJ. 2014. A Diel Flux Balance Model Captures Interactions between Light and Dark Metabolism during Day-Night Cycles in C3 and Crassulacean Acid Metabolism Leaves. *Plant Physiology* 165, 917–929.
- Cushman JC. 2001. Crassulacean Acid Metabolism. A Plastic Photosynthetic Adaptation to Arid Environments. *Plant Physiology* 127, 1439–1448.
- Cushman JC, Borland AM. 2002. Induction of Crassulacean acid metabolism by water limitation. *Plant, Cell and Environment* 25, 295–310.
- Ebrahim A, Lerman JA, Palsson BO, Hyduke DR. 2013. COBRAPy: CONstraints-Based Reconstruction and Analysis for Python. *BMC Systems Biology* 7, 74.
- Lüttge U. 2004. Ecophysiology of Crassulacean Acid Metabolism (CAM). *Annals of Botany* 93, 629–652.
- Mahadevan R, Schilling CH. 2003. The effects of alternate optimal solutions in constraint-based genome-scale metabolic models. *Metabolic engineering*, 5, 264-276.
- Shameer S, Baghalian K, Cheung CYM, Ratcliffe RG, Sweetlove LJ. 2018. Computational analysis of the productivity potential of CAM. *Nature Plants* 4, 165–171.
- Silvera K, Neubig KM, Whitten WM, Williams NH, Winter K, Cushman JC. 2010. Evolution along the crassulacean acid metabolism continuum. *Functional Plant Biology* 37, 995.
- Sipes DL, Ting IP. 1985. Crassulacean Acid Metabolism and Crassulacean Acid Metabolism Modifications in *Peperomia camptotricha*. *Plant Physiology* 77, 59–63.
- Ting IP. 1985. Crassulacean Acid Metabolism. *Annual Review of Plant Physiology* 36, 595–622.
- Winter K, Smith JAC. 1996a. An introduction to crassulacean acid metabolism. Biochemical principles and ecological diversity. In: Winter K, Smith JAC, eds. *Crassulacean acid metabolism. Biochemistry, ecophysiology and evolution. Ecological Studies, Vol. 114.* Berlin, Heidelberg, New York: Springer Verlag, 1-13.
- Winter K, Smith JAC. 1996b. Crassulacean acid metabolism: current status and perspectives. In: Winter K, Smith JAC, eds. *Crassulacean acid metabolism. Biochemistry, ecophysiology and*

evolution. *Ecological Studies*, Vol. 114. Berlin, Heidelberg, New York: Springer Verlag, 389-426.

Winter K. 2019. Ecophysiology of constitutive and facultative CAM photosynthesis. *Journal of Experimental Botany* 70, 6495-6508.

Tables

Table 1: Sets of constraints for modelling C₃, CAM, CAM cycling and CAM idling. Phloem export rate was set based on the predicted value of C₃ plants in Shameer et al. (2018). RuBisCO carboxylase:oxygenase ratio was set to 3:1 when stomata is opened, and 5.15:1 when stomata is closed based on Shameer et al. (2018).

Constraints ($\mu\text{mol m}^{-2} \text{s}^{-1}$)	C₃	CAM	CAM Cycling	CAM Idling
Phloem export	0.259	0.259	0.259	0
CO ₂ exchange (light)	Unconstrained	0	Unconstrained	0
CO ₂ exchange (dark)	Unconstrained	Unconstrained	0	0
O ₂ exchange (light)	Unconstrained	0	Unconstrained	0
O ₂ exchange (dark)	Unconstrained	Unconstrained	0	0
RuBisCO carboxylase:oxygenase ratio (light)	3:1	5.15:1	3:1	5.15:1
RuBisCO carboxylase:oxygenase ratio (dark)	3:1	3:1	5.15:1	5.15:1

Table 2. Fluxes related to energetics and metabolic accumulation predicted in the model simulations of C₃, CAM cycling, CAM idling and CAM. Photon demand and the productions of ATP and NADPH by photosynthetic light reaction are flux values from the light period. A positive value of metabolite accumulation denotes a net accumulation in the light period; negative value of metabolite accumulation denotes a net accumulation in the dark period. All values are in the units of $\mu\text{mol m}^{-2} \text{s}^{-1}$.

	C ₃	CAM	CAM cycling	CAM idling
Photon demand	199.40	213.39	209.04	57.484
ATP production by photosynthetic light reaction	64.09	68.59	67.19	18.48
NADPH production by photosynthetic light reaction	46.80	51.38	49.15	14.06
ATP production by the mitochondrial ETC (light)	14.49	37.86	19.66	11.57
ATP production by the mitochondrial ETC (dark)	7.20	13.20	8.39	8.27
Starch accumulation	0.86	8.14	2.35	1.94
Malate accumulation	0.04	-14.13	-2.84	-2.92

Figure Legends

Figure 1. Core sets of metabolic fluxes in the four modes of photosynthesis modelled: (A) C₃, (B) CAM, (C) CAM cycling and (D) CAM idling. The width of the arrows represents the magnitude of the reaction flux according to the scale on the bottom of the figure in $\mu\text{mol m}^{-2} \text{s}^{-1}$. The photorespiratory pathway is shown in chloroplast for simplicity, which in reality spans multiple compartments. Flux from 3-phosphoglycerate to PEP was taken as the flux for glycolysis and gluconeogenesis. Flux for succinate dehydrogenase was taken as the TCA cycle flux. RuBisCO carboxylase flux was taken as the flux through the Calvin-Benson cycle.

Figure 2. Model predictions of metabolic changes along the C₃-CAM continuum, as modelled by varying CO₂ exchange during the light period. (A) Accumulation of starch (dots) and malate (crosses), (B) Dark period PEPC flux in the dark period (dots) and malate carboxylation flux as the sum of fluxes of PEPC and malic enzyme in the light period (crosses), (C) Photon intake in the light period, (D) ATP synthesis in the light period by plastidial ATP synthase (dots) and mitochondrial ATP synthase (crosses), (E) Proportion of light period ATP synthesis by the mitochondrial ATP synthase, (F) Fluxes of RuBisCO carboxylase (dots) and oxygenase (crosses), (G) Fluxes through the TCA cycle (taken as the flux of succinate dehydrogenase; dots) and the mitochondrial ETC (taken as the flux of NADH dehydrogenase; crosses) in the dark period, and (H) flux through the OPPP (taken as the sum of fluxes of plastidial and cytosolic glucose 6-phosphate dehydrogenases) in the dark period.

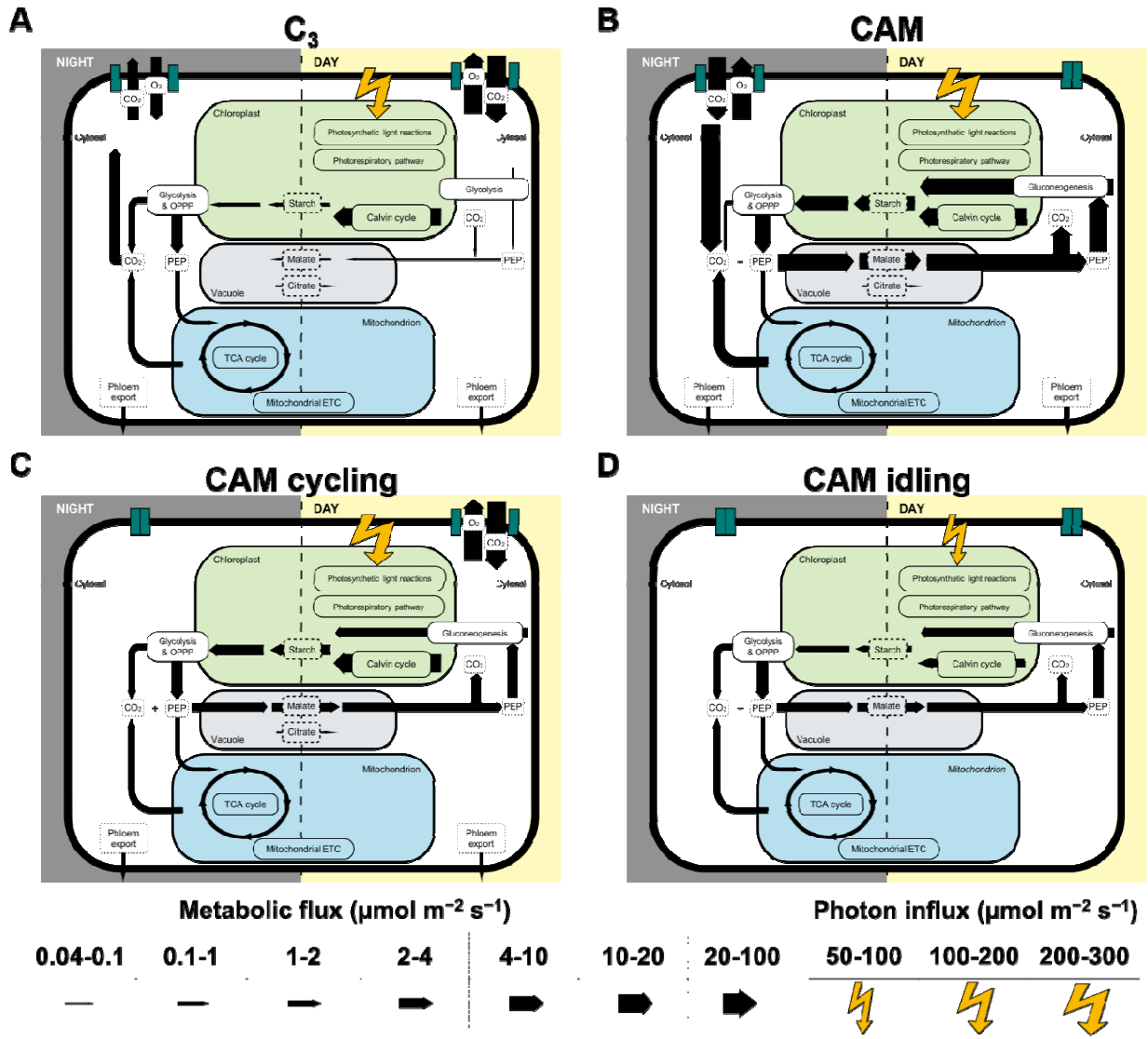


Figure 1. Core sets of metabolic fluxes in the four modes of photosynthesis modelled: (A) C₃, (B) CAM, (C) CAM cycling and (D) CAM idling.

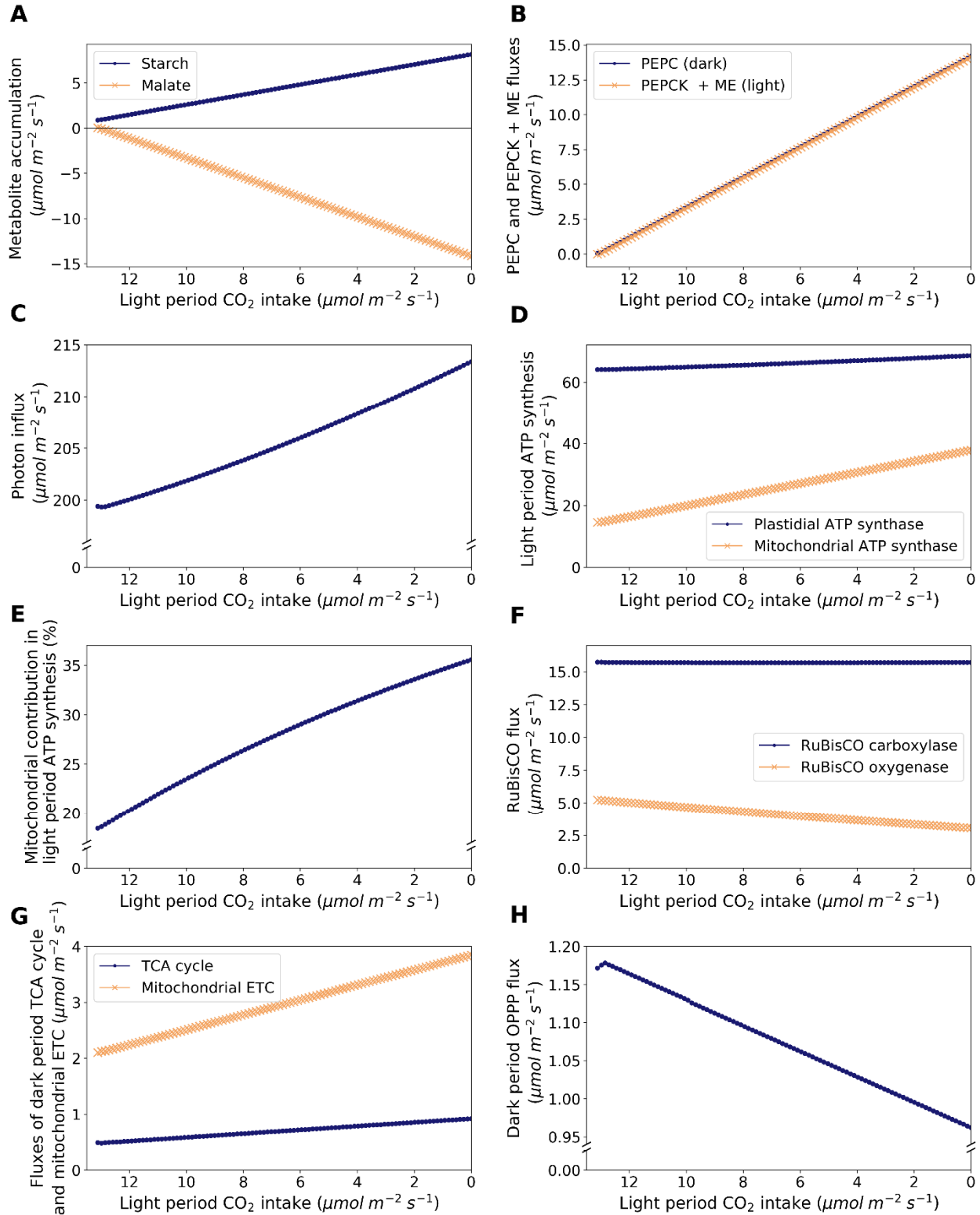


Figure 2. Model predictions of metabolic changes along the C₃-CAM continuum, as modelled by varying CO₂ exchange during the light period.